Metal–Organic Frameworks

International Edition: DOI: 10.1002/anie.201606185
German Edition: DOI: 10.1002/ange.201606185

Complete Transmetalation in a Metal–Organic Framework by Metal Ion Metathesis in a Single Crystal for Selective Sensing of Phosphate Ions in Aqueous Media

*K S Asha, Rameswar Bhattacharjee, and Sukhendu Mandal**

Dedicated to Professor Animesh Chakravorty

Abstract: *A complete transmetalation has been achieved on a barium metal–organic framework (MOF), leading to the isolation of a new Tb-MOF in a single-crystal (SC) to single-crystal (SC) fashion. It leads to the transformation of an anionic framework with cations in the pore to one that is neutral. The mechanistic studies proposed a core–shell metal exchange through dissociation of metal–ligand bonds. This Tb-MOF exhibits enhanced photoluminescence and acts as a selective sensor for phosphate anion in aqueous medium. Thus, this work not only provides a method to functionalize a MOF that can have potential application in sensing but also elucidates the formation mechanism of the resulting MOF.*

The synthesis and design of MOFs has had a very rapid and extensive growth during past years,[1,2] but control over MOF structure is always difficult owing to many factors that affect their assembly.[3] The MOFs can easily swap their constituents with the surrounding medium through post-synthetic modification and can create novel structures with induced properties.[4] The cation and/or ligand exchange are a powerful technique for designing new materials, and this process offers an alternative and effective route for accessing materials when the conventional direct synthesis fails.[5] These post-synthetic treatments may occur without altering the topology and structural integrity. Since this involves the formation and cleavage of metal–ligand bonds, usually MOFs with labile metal–ligand bonds undergo such transformation.[6]

Although metal exchange in MOFs are simple and convenient, the complete transmetalation at the metal node of the SBU (secondary building unit) is scarce. There are several factors, such as pore diameter and framework flexibility, ionic radii and coordination modes of the exchanged metals, electronegativity difference between the incoming and leaving metals, and the solvent control the ion exchange process.[7] There are reports on metal exchange between transition metals or transition metal and main group metal.[8] According to our knowledge, there are no reports of metal exchange between alkaline earth and rare earth metal ions.

Recently we reported a three-dimensional porous MOF,[9] $[H_2N(CH_3)_2][Ba(H_2O)(BTB)]$, **1**, constructed from an alkaline earth metal ion and 1,3,5-benzenetribenzoic acid ligand. Herein we show that this compound undergoes metal exchange with the Tb^{3+} ion at the metal node in a SC to SC fashion to form $[Tb(H_2O)(BTB)]$ (**2**). We have monitored this transmetalation process using the techniques like fluorescence microscopy, ICP-AES, and SEM-EDAX. Both the parent and daughter MOFs are isostructural. The ability to have high coordination number and comparable ionic radii guide us to try the metal exchange using Tb^{3+} ions.[10] Tb^{3+} ions are useful as luminescent probes, and the Tb^{3+}-centered emission can be sensitized by molecules with π-electrons. Thus, the replacement of Ba by Tb metal ions may induce attractive enhanced emission properties. Anion recognition and separation is currently a very active topic of research because various anions play a central role in chemical and biological processes. The inorganic–organic hybrid porous MOFs could be excellent host receptors to recognize and separate anionic species based on their size, geometry, basicity, and binding ability under ambient conditions.[11] In present work the transmetalated MOF is found to be useful for the selective sensing of phosphate anions in aqueous medium with a detection limit of 4×10^{-5} M (6.56 ppm).

Compound **2** was obtained by the cation-exchange reaction at the SBU by immersing the crystals of **1** in DMF solution of $Tb(NO_3)_2{\cdot}5H_2O$ for 24 h (see the Supporting Information). The whole exchange process was followed visually by fluorescence microscopy, and no complete crystal dissolution was observed, although the final crystals have different shape and size (Figure 1; Supporting Information, Figure S1). This partially rules out the possible dissolution–recrystallization mechanism. The possible core–shell metal exchange through a dissociative mechanism is assumed as the exchange proceeds from the surface of the crystals to the core (Figure 2a; Supporting Information, Figure S2). The formation of **2** from the corresponding reagents using direct conventional solvothermal method was unsuccessful (Supporting Information, Table S3). The supernatant after the metal exchange was treated with BTB ligand at 100 °C and the crystals of **1** were formed whereas no crystals were formed when treated with excess Ba^{2+} and heated at 100 °C (Support-

[*] K. S. Asha, Dr. S. Mandal
School of Chemistry, Indian Institute Science Education and Research, Thiruvananthapuram (India)
E-mail: sukhendu@iisertvm.ac.in
R. Bhattacharjee
Department of Spectroscopy
Indian Association for the Cultivation of Science
Jadavpur, Kolkata-700032 (India)

Supporting information for this article can be found under: http://dx.doi.org/10.1002/anie.201606185.

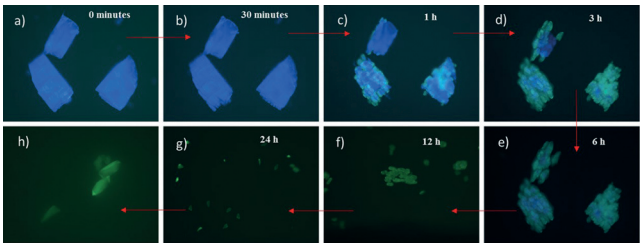

Figure 1. A real time analysis of single crystal to single crystal transformation during metal exchange reaction in compound **1**.

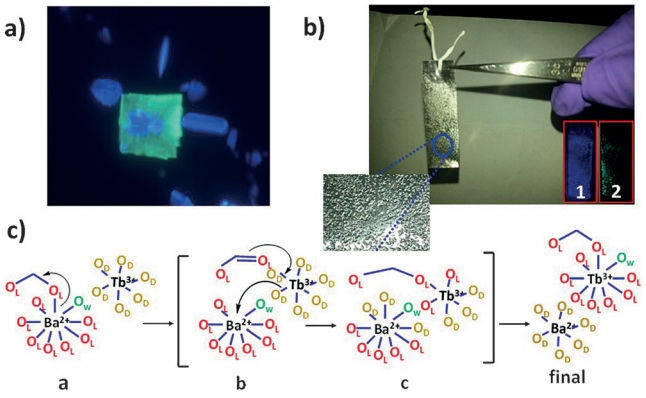

Figure 2. a) Microscopic image of crystal showing the metal exchange from surface to core b) the photograph of crystals grown on the Al foil and that under UV light (inset) c) the proposed dissociative mechanism of metal metathesis in crystals, O_L is carboxylic oxygen of ligand, Ow is the oxygen from the coordinated water molecule, and O_D is the oxygen from solvent molecule.

ing Information, Figure S4). The reverse exchange could be observed at 100 °C in the presence of excess Ba^{2+} ion and trace amount of diluted HCl. We have grown the single crystals of **1** on aluminum foil and then carried out Tb^{3+} exchange on it (Figure 2b; Supporting Information, Figure S5).

Both the compounds crystallize in same space group with similar structural connectivity (Supporting Information, Figure S6).[23] For the case of **1** an extra framework cation, DMA (dimethylammonium) is present, but it is absent in **2**. In both cases the metal ion is a nine-coordinate MO_9 unit that is linked through oxygen atoms edge-wise to form a one-dimensional zig-zag chain with infinite M-O-M bonds along *a*-axis. These chains are linked through carboxylate moiety to form a three-dimensional structure (Supporting Information, Figures S6–S9). The Ba–O bond lengths are in the range of 2.752–2.939 Å (av. 2.8291 Å) whereas Tb–O distances are in the range of 2.704–2.864 Å (Av. 2.7871 Å) (Supporting Information, Table S10). The excessive strain in the framework due to the nine-coordinate metal node is reduced by the introduction of the smaller ion (ionic radii Tb^{3+}: 118 pm vs. Ba^{2+}: 135 pm). The metal sites that are coordinately saturated undergo complete cation exchange; they might do so because their weak field ligands dissociate readily. The shorter Tb–O bond distance compared to the Ba–O bond length suggests the higher stability of the framework in **2** and the equilibrium shifts more towards **2** during the metal exchange. The symmetric COO^- stretching peak in the IR spectrum at 1411 cm^{-1} is shifted to 1382 cm^{-1} by Tb^{3+} exchange (Supporting Information, Figure S11). This may be due to the higher affinity of Tb^{3+} to carboxylate oxygen atom over Ba^{2+}.

The size of solvation sphere impacts the rate of substitution and it plays a mechanistic role apart from shuttling the solvated cations through pores to the vicinity of SBU. In the present work, the metal exchange was successful only in DMF solvent, and it was found to fail in methanol and acetone. A dissociative mechanism is assumed to take place, since the bond between the metal and the organic linker in the MOF is not too strong and can be broken, especially if it is displaced by the solvent. The initial step involves the active participation of the DMF, and it induces the breaking of Ba–O bond resulting in a swinging carboxylate group. This group is then free to coordinate to a nearby $Tb(DMF)_n^{3+}$. The replacement of one of the carboxylate unit at the Ba center by DMF yielding an intermediate, then the COO^- moiety successively coordinates to $Tb(DMF)_n^{3+}$, leading to the next intermediate.[12] Finally, after successive steps, the complete exchange of metal ion occurs (Figure 2c).

The metal substitution experiments were carried out to understand the thermodynamics and kinetics of metal exchange process. For this we first fixed the metal ion ratio as 1:1 (M/M′; that is the mole of Ba-MOF: mole of $Tb(NO_3)_2$ used for PSM) and monitored the amount of metal exchange (M′/M represents the percentage of Tb^{3+} incorporated, and M/M′ represents Ba^{2+} removed from the MOF) at different time intervals (Figure 3a; Supporting Information, Figure S12, Table S13). The thermodynamic studies were carried out by fixing the reaction time (time for given metal exchange) as 10 h and varying the metal ion ratio (M/M′) to

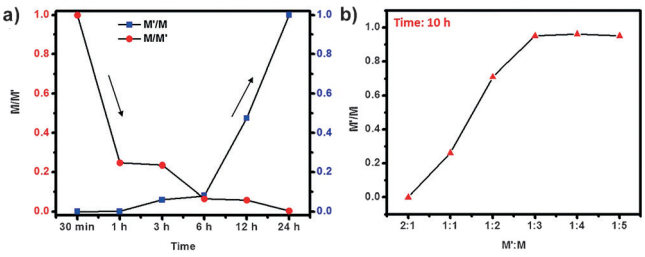

Figure 3. a) The kinetic and b) the thermodynamic studies of metal exchange in compound **1**.

1:1, 1:2, 1:3, 1:4, and 1:5 (Figure 3b). We have observed that Ba^{2+} ion is completely exchanged by Tb^{3+} in 10 h when the concentration of M′ reaches three equivalents of that of M. No change was observed for the higher concentration of M′.

The PXRD patterns for **1** and **2** are almost identical and thus it confirms that the bulk samples are isostructural (Supporting Information, Figure S14). Due to the absence of DMA cation, the weight loss in thermogravimetric analysis data for compound **2** is lesser compared to **1** (Supporting Information, Figure S15a). This is manifested in DSC measurement where no transition was observed at around 200 °C, which might be due to the absence of extra framework cation

(Supporting Information, Figure S15b). Compound **2** exhibits strong emission in visible region (at 486, 541, 583, and 618 nm can be assigned to the $^5D_4 \rightarrow {}^7F_6$, $^5D_4 \rightarrow {}^7F_5$, $^5D_4 \rightarrow {}^7F_4$, and $^5D_4 \rightarrow {}^7F_3$ transitions) along with a weak emission band at 370 nm owing to ligand upon excitation at 320 nm (Supporting Information, Figure S16).[13]

Taking the advantages of unique optical properties, we have used **2** for the detection of pollutant anions as these can be selectively detected by weak interactions between guest anions and framework. The detection of phosphate anion is important in biological systems and also environmentally.[14] The change in fluorescent intensity of **2** was monitored with several pollutant anions, and it showed that **2** can selectively detect phosphate anion (Figure 4b). The intensity of emission peaks due to LMCT were found to be quenched by the increase of phosphate ion concentration and the contact time, whereas the intensity of the peak at 370 nm was found to be

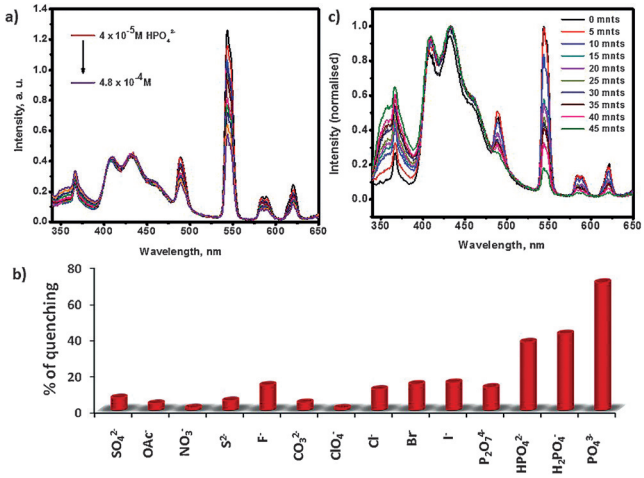

Figure 4. The change in fluorescence intensity of compound **2** a) as a function of the concentration of phosphate anion, b) the selective detection of phosphate anion over other anions using compound **2**, and c) as a function of contact time of phosphate anion.

enhanced (Figure 4a,c). The high selectivity and specificity is necessary for a real sample detection, so we have measured the emission spectra by addition of other pollutant anions (Cl^-, Br^-, F^-, I^-, OAc^-, ClO_4^-, SO_4^{2-}, S^{2-}, NO_2^-, NO_3^-, and CO_3^{2-}) to the Tb–O phosphate system and no significant fluorescence change was observed (Supporting Information, Figures S17 and S18), which confirm that the Tb-MOF is active for the selective detection of phosphate with good anti-interference ability to co-existing anions. As a control experiment, the capability of free BTB ligand and **1** for phosphate sensing was tested. No specific fluorescence response was observed, and it indicated that the coordination of Tb–O cluster to the BTB ligand has a key role for the selective detection of phosphate anion (Supporting Information, Figure S19). To determine the sensitivity of compound **2** for the detection of phosphate, fluorescence titration spectra with a different concentration of phosphate were performed. The fluorescence intensity of **2** gradually decreases upon gradual addition of phosphate anions. The fluorescence sensing of **2** has a good linear correlation ($R^2 = 0.973$) in the range of 40–400 μM (Supporting Information, Figure S20). The limit of detection was estimated to be 35 μM. It is the detection requirement of phosphate discharge criteria in the water environment, reported to be around 6.4–320 μM.[15]

It is a challenge to select anions selectively in aqueous medium owing to their strong hydration effects. Among the anions, phosphate has a relatively high hydration energy owing to central phosphorus being surrounded by four oxygen atoms and is highly hydrophilic in nature with a high charge-to-radius ratio.[16] There are a few factors that affect the anion binding, such as geometry and charge of the anion, nature of solvent medium, non-covalent interactions between the metal cluster, and the anion and finally the lability of metal center.[17–19] The anions with trigonal or tetragonal geometry make a complementary and competitive coordination interaction with the carboxylate ligand bonded to the Tb–O cluster, whereas other anions with spherical or linear shape contribute less affinity towards the metal center (Supporting Information, Figure S21). Thus, Tb–O bonds between the cluster and carboxylate groups could be partially broken and replaced by a phosphate anion. The more electronegative P–O bond interacts more strongly with the Tb^{3+} ion. The pyrophosphate ion could not be detected, as it is bulkier compared to simple phosphate ion. The phosphate ion binds to metal center through possible hydrogen bonding with the coordinated water molecule. We also carried out a quenching experiment using anions dissolved in isopropanol/water (50:1 v/v) mixture and it was observed that the quenching efficiency is decreased (Supporting Information, Figure S22). This implies that an aqueous medium is also essential for selective phosphate sensing.

The selective detection of phosphate anion may be due to the weak interactions of P–O bonds of phosphate anion with Tb–O cluster and thus it may affect the electron transfer between Tb coordination sphere and BTB ligand (Supporting Information, Figure S23). The vibrational absorption band associated with the stretching of carboxylate C–O bonds become weaker or even disappears at high level of phosphate anion (Supporting Information, Figure S24). For a better understanding of the possible mechanism of the selective sensing of phosphate by compound **2**, X-ray photoelectron spectroscopy (XPS) was carried out to underscore the interaction between phosphate and framework of **2**. In the XPS data, the slight shift of binding energy to a higher energy might be due to the interaction of phosphate groups with the Tb center (Supporting Information, Figure S25). The more electronegative P–O bond leads to the loss of electron density at Tb, which in turn raises its 3d electrons binding energy.

To provide more depth on this mechanistic aspect we have performed theoretical investigation. To make the computation tractable, the structure was suitably modeled. Geometry optimization were performed using universal force field (UFF)[20] as implemented in Gaussian 09.[21] The optimized geometry of the parent and phosphate substituted MOF are shown in Figure 5 and the Supporting Information, Figure S26. It is observed that the phosphate is binding in a bridging fashion similar to the carboxylate group but with comparatively short Tb–O distance of 2.2 Å. This shorter

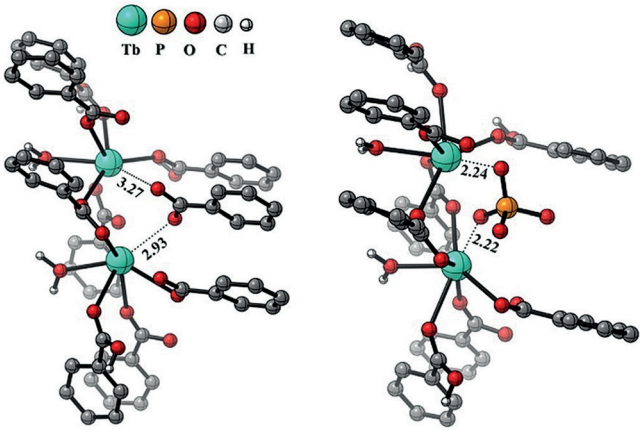

Figure 5. The comparison of strength of binding between the carboxylate and phosphate ion to metal center in MOF.

bond distances is attributed to the higher interaction of PO_4^{3-} with the MOF. Moreover, in the hydrolysis enzyme where Zn^{2+} center is bound the optimized Zn–O–P distance is 2.24 Å and that for Zr–O–P in NU-1000 is 2.22 Å close to Tb–O–P distance in present case.[22]

In summary, we have carried out post-synthetic transmetalation via SC to SC fashion between Ba^{2+}- and Tb^{3+}-based MOFs. ICP-AES data shows that Ba^{2+} was completely exchanged by Tb^{3+} ion. Based on fluorescence microscopy images, we have proposed the metal exchange through a possible dissociative mechanism. The transmetalated Tb MOF detects phosphate anion in aqueous medium selectively with good anti-interference ability to co-existing anions. Specific geometry, high charge to radius ratio, and strong hydrophilicity of the phosphate anion might be the reason for selectivity. XPS data and theoretical calculation supports the interaction of phosphate to the MOF. Thus, this work provides a strategy to develop a chemical sensor via post-synthetic modification.

Acknowledgements

We acknowledge Science and Engineering Research Board (SERB), Govt. of India, through a grant SB/S1/IC-14/2013 for funding. We acknowledge IISc nanocentre for XPS measurements and SAIF, IIT Bombay for ICP-AES measurements. We also acknolwedge Dr. Nishant KT for fluorescence microscopy facility. We are grateful to Prof. V. Ramakrishnan for encouragement and support. AKS acknowledges CSIR for fellowship.

Keywords: metal–organic frameworks · metathesis · SC to SC transformation · phosphate · selective sensing

How to cite: *Angew. Chem. Int. Ed.* **2016**, *55*, 11528–11532
Angew. Chem. **2016**, *128*, 11700–11704

[1] a) H. Li, M. Eddaoudi, M. O'Keeffe, O. M. Yaghi, *Nature* **1999**, *402*, 276–279; b) G. Férey, *Chem. Soc. Rev.* **2008**, *37*, 191–214; c) J. R. Long, O. M. Yaghi, *Chem. Soc. Rev.* **2009**, *38*, 1213–1214; d) H. Furukawa, K. E. Cordova, M. O'Keeffe, O. M. Yaghi, *Science* **2013**, *341*, 974–986; e) H.-C. Zhou, S. Kitagawa, *Chem. Soc. Rev.* **2014**, *43*, 5415–6010.

[2] a) E. Coronado, J. R. Galán-Mascarós, C. J. Gómez-García, V. Laukhin, *Nature* **2000**, *408*, 447–449; b) E. Pardo, C. Train, G. Gontard, K. Boubekeur, O. Fabelo, H. Liu, F. Lloret, K. Nakagawa, H. Tokoro, S.-i. Ohkoshi, M. Verdaguer, *J. Am. Chem. Soc.* **2011**, *133*, 15328–15331; c) G.-C. Xu, W. Zhang, X.-M. Ma, Y.-H. Chen, L. Zhang, H.-L. Cai, Z.-M. Wang, R.-G. Xiong, S. Gao, *J. Am. Chem. Soc.* **2011**, *133*, 14948–14951; d) E. Pardo, C. Train, H. Liu, L.-M. Chamoreau, B. Dkhil, K. Boubekeur, F. Lloret, K. Nakatani, H. Tokoro, S.-i. Ohkoshi, M. Verdaguer, *Angew. Chem. Int. Ed.* **2012**, *51*, 8356–8360; *Angew. Chem.* **2012**, *124*, 8481–8485.

[3] M. G. Goesten, F. Kapteijn, J. Gascon, *CrystEngComm* **2013**, *15*, 9249–9257.

[4] a) C. K. Brozek, M. Dincă, *Chem. Soc. Rev.* **2014**, *43*, 5456–5467; b) K. Min, F. C. John, S. Yongxuan, A. P. Kimberly, M. C. Seth, *Chem. Sci.* **2012**, *3*, 126–130.

[5] a) M. Kim, J. F. Cahill, H. Fei, K. A. Prather, S. M. Cohen, *J. Am. Chem. Soc.* **2012**, *134*, 18082–18088; b) F. G. Adam, S. Elena, L. M. Sky, J. V. John, *J. Phys. Chem. A* **2013**, *117*, 3771–3776; c) F. Honghan, F. C. John, A. P. Kimberly, M. C. Seth, *Inorg. Chem.* **2013**, *52*, 4011–4016; d) L. Tao, T. K. Mark, A. D. Evan, N. B. Maike, L. R. Nathaniel, *J. Am. Chem. Soc.* **2013**, *135*, 11688–11691; e) S. Das, H. Kim, K. Kim, *J. Am. Chem. Soc.* **2009**, *131*, 3814–3815.

[6] a) Z. Wang, S. M. Cohen, *J. Am. Chem. Soc.* **2007**, *129*, 12368–12369; b) G. Mukherjee, K. Biradha, *Chem. Commun.* **2012**, *48*, 4293–4295.

[7] a) M. Lalonde, W. Bury, O. Karagiaridi, Z. Brown, J. T. Hupp, O. K. Farha, *J. Mater. Chem. A* **2013**, *1*, 5453–5468; b) C. K. Brozek, L. Bellarosa, T. Soejima, T. Clark, V. N. López, M. Dincă, *Chem. Eur. J.* **2014**, *20*, 6871–6874.

[8] a) M. Dincă, J. R. Long, *J. Am. Chem. Soc.* **2007**, *129*, 11172–11176; b) L. Mi, H. Hou, Z. Song, H. Han, H. Xu, Y. Fan, S.-W. Ng, *Cryst. Growth Des.* **2007**, *7*, 2553–2561.

[9] K. S. Asha, M. Makkitaya, A. Sirohi, L. Yadav, G. Sheet, S. Mandal, *CrystEngComm* **2016**, *18*, 1046–1053.

[10] a) T. Devic, C. Serre, N. Audebrand, J. Marrot, G. Férey, *J. Am. Chem. Soc.* **2005**, *127*, 12788–12789; b) A. de Bettencourt-Dias, *Inorg. Chem.* **2005**, *44*, 2734–2741.

[11] a) J.-P. Ma, Y. Yu, Y.-B. Dong, *Chem. Commun.* **2012**, *48*, 2946–2948; b) H. Xu, C.-S. Cao, B. Zhao, *Chem. Commun.* **2015**, *51*, 10280–10283.

[12] L. Bellarosa, C. K. Brozek, M. G. Melchor, M. Dincă, N. López, *Chem. Mater.* **2015**, *27*, 3422–3429.

[13] a) P. Mahata, K. V. Ramya, S. Natarajan, *Chem. Eur. J.* **2008**, *14*, 5839–5850; b) P. Mahata, K. V. Ramya, S. Natarajan, *Dalton Trans.* **2007**, *36*, 4017–4026; c) D. K. Singha, S. Bhattacharya, P. Majee, S. K. Mondal, M. Kumar, P. Mahata, *J. Mater. Chem. A* **2014**, *2*, 20908–20915.

[14] a) J. Yang, Y. Dai, X. Zhu, Z. Wang, Y. Li, Q. Zhuang, J. Shi, J. Gu, *J. Mater. Chem. A* **2015**, *3*, 7445–7452; b) H. Xu, Y. Xiao, X. Rao, Z. Dou, W. Li, Y. Cui, Z. Wang, G. Qian, *J. Alloys Compd.* **2011**, *509*, 2552–2554.

[15] a) S. A. Rodrigues, S. S. Caldas, E. G. Primel, *Anal. Chim. Acta* **2010**, *82*, 1157–1161; b) K. Wygladacz, Y. Qin, W. Wroblewski, E. Bakker, *Anal. Chim. Acta* **2008**, *614*, 77–84; c) W. C. Mak, C. Chan, J. Barford, R. Renneberg, *Biosens. Bioelectron.* **2003**, *19*, 233–237.

[16] P. D. Beer, P. A. Gale, *Angew. Chem. Int. Ed.* **2001**, *40*, 486–516; *Angew. Chem.* **2001**, *113*, 502–532.

[17] A. Ojida, H. Nonaka, Y. Miyahara, S.-i. Tamaru, K. Sada, I. Hamachi, *Angew. Chem. Int. Ed.* **2006**, *45*, 5518–5521; *Angew. Chem.* **2006**, *118*, 5644–5647.

[18] J. W. Steed, *Chem. Soc. Rev.* **2009**, *38*, 506 – 519.
[19] J.-M. Bai, L. Zhang, R.-P. Liang, J.-D. Qiu, *Chem. Eur. J.* **2013**, *19*, 3822 – 3826.
[20] A. K. Rappe, C. J. Casewit, K. S. Colwell, W. A. Goddard, W. M. Skiff, *J. Am. Chem. Soc.* **1992**, *114*, 10024 – 10035.
[21] M. J. Frisch, Gaussian 09; Gaussian, Inc: Pittsburgh, PA, **2009**. Full citations are available in the Supporting Information.
[22] J. E. Mondloch, M. J. Katz, W. C. Isley, P. Ghosh, P. Liao, W. Bury, G. W. Wagner, M. G. Hall, J. B. DeCoste, G. W. Peterson, R. Q. Snurr, C. J. Cramer, J. T. Hupp, O. K. Farha, *Nat. Mater.* **2015**, *14*, 512 – 516.
[23] CCDC 1449939 (**1**, RT), 1450180 (**1**, 150 K), and 1449885 (**2**) contain the supplementary crystallographic data for this paper. These data are provided free of charge by The Cambridge Crystallographic Data Centre.

Received: June 26, 2016
Published online: August 12, 2016

